



OPEN

SUBJECT AREAS:

SYNTHESIS OF  
GRAPHENE

ELECTROCHEMISTRY

# Role of Peroxide Ions in Formation of Graphene Nanosheets by Electrochemical Exfoliation of Graphite

Kodepelly Sanjeeva Rao, Jaganathan Senthilnathan, Yung-Fang Liu &amp; Masahiro Yoshimura

Received  
25 October 2013Accepted  
4 February 2014Published  
28 February 2014Correspondence and  
requests for materials  
should be addressed to  
M.Y. (yoshimur@mail.  
ncku.edu.tw)

Promotion Centre for Global Materials Research (PCGMR), Department of Material Science and Engineering, National Cheng Kung University, Tainan, Taiwan.

**This study demonstrates a facile, mild and environmentally-friendly sustainable (soft processing) approach for the efficient electrochemical exfoliation of graphite using a sodium hydroxide/hydrogen peroxide/water (NaOH/H<sub>2</sub>O<sub>2</sub>/H<sub>2</sub>O) system that can produce high-quality, anodic few-layer graphene nanosheets in 95% yield at ambient reaction conditions. The control experiment conducted using NaOH/H<sub>2</sub>O revealed the crucial role of H<sub>2</sub>O<sub>2</sub> in the exfoliation of graphite. A possible exfoliation mechanism is proposed. The reaction of H<sub>2</sub>O<sub>2</sub> with hydroxyl ions (HO<sup>-</sup>) leads to the formation of highly nucleophilic peroxide ions (O<sub>2</sub><sup>2-</sup>), which play a crucial role in the exfoliation of graphite via electrochemical-potential-assisted intercalation and strong expansion of graphite sheets.**

The excellent mechanical, electrical, thermal, optical properties and high specific surface area of graphene, and manipulation of these properties via chemical functionalization/surface modification makes it rapid growing field in material science. High-quality graphene materials and their composites with several structures such as metal-organic frameworks, polymers, biomaterials, organic crystals, and inorganic nanostructures, are used in various emerging fields. The development of efficient methods for the preparation<sup>1–5</sup> of these materials has received a lot of interest due to their potential applications. Several synthetic approaches are reported such as chemical vapor deposition (CVD)<sup>6–7</sup>, micromechanical exfoliation<sup>4,5</sup>, and epitaxial growth on SiC<sup>3,4</sup>, solution route wet chemical exfoliation<sup>4,8</sup>, sonochemical liquid-phase exfoliation<sup>4,9</sup>, and volatile agents promote intercalation-expansion<sup>1,3</sup>. Solution processing<sup>1–4,9–13</sup> is of interest due to low cost and environmental friendliness. Recently, the direct electrochemical exfoliation of graphite into low-defect graphene nanosheets has been reported. Several electrolytes, such as ionic liquids<sup>14–16</sup>, acids<sup>17–20</sup>, and high-temperature (600°C) molten salts<sup>21</sup> have been used. The intercalation of Li ions in propylene carbonate electrolyte followed by either prolonged (>10 h) sonication<sup>22</sup> or tetra-*n*-butyl ammonium-assisted electrochemical activation<sup>23</sup> has been reported. Alanyaloglu et al. presented a method<sup>24</sup> that use sodium dodecyl sulfate as the intercalation agent for the synthesis of graphene sheets with a controlled thickness. Zhou et al.<sup>25</sup> studied the synthesis of few-layer graphene using Na<sup>+</sup>/dimethylsulfoxide complexes as intercalation agents and the subsequent addition of thionin acetate for exfoliation. They have proposed that, these electrochemical exfoliation methods have several advantages, including easy processing of graphene and functionalized graphene. However, these methods have major shortcomings, including the requirement of strong (non-soft) chemicals such as ionic liquids and/or hazardous reagents such as phosphoric acid, lithium perchlorate, and 3-(aminopropyl) triethoxy silane, additional steps, high voltages, low quality, and multilayer graphene formation.

The rapid exfoliation of graphite powder using a mixture of chlorosulfonic acid (CSA) and H<sub>2</sub>O<sub>2</sub> for the synthesis of few-layer graphene has also been reported<sup>26</sup> by Lu et al. However, the usage of large quantities of CSA (6 mL) and H<sub>2</sub>O<sub>2</sub> (3 mL) for only 50 mg of graphite exfoliation is a major drawback. The formation of HCl fumes via the exothermic reaction of CSA with H<sub>2</sub>O<sub>2</sub> further complicates the process. Additionally, CSA is a hazardous<sup>27</sup> compound and thus highly incompatible with health and environmental standards. Sole CSA solution requires prolonged (12 h) centrifugation for graphene formation via graphene exfoliation<sup>28</sup>.

Considering the disadvantages of all these approaches, the present study proposes a process that allows the electrochemical exfoliation of graphite by using a significantly lower toxicity NaOH<sup>29</sup>. The NaOH-induced electrochemical reduction<sup>30</sup> of preformed oxygen functional groups of graphene is an additional benefit. H<sub>2</sub>O<sub>2</sub> has selected to go along with NaOH in the exfoliation process due to its remarkable advantages, such as low cost, environmental-friendliness<sup>31</sup>, versatility, selectivity, wide availability, safety, and effectiveness as a reagent. The

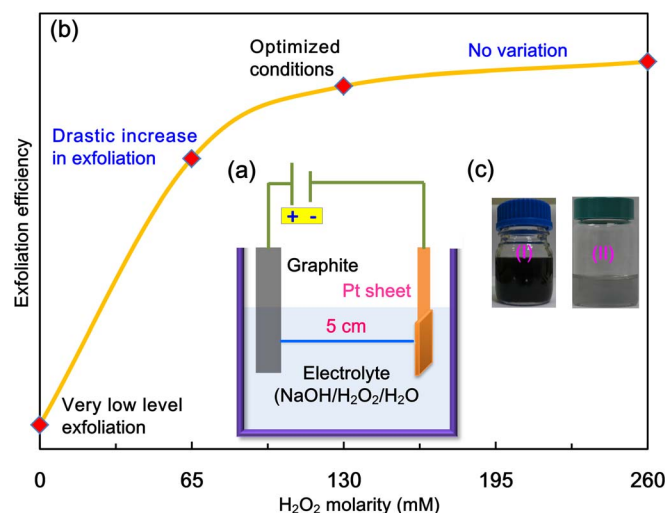


**Figure 1** | Electrochemical exfoliation process. (a) diagram of experimental setup (b) efficiency of exfoliation versus hydrogen peroxide molarity and (c) photograph of exfoliated AFLG directly in electrolyte solution (I) and dispersed in dimethyl formamide (II) after purification.

present study thus developed a promising facile soft processing<sup>32–35</sup> approach that uses NaOH/H<sub>2</sub>O<sub>2</sub>/H<sub>2</sub>O mild<sup>36,37</sup> system for the electrochemical exfoliation of graphite. A systematic study on the efficiency of the exfoliation process, the quality of processed graphene, and the stability of dispersed solutions was conducted. These materials are characterized and a possible exfoliation mechanism is proposed.

## Results

A schematic illustration of the experimental setup is shown in Figure 1a. The setup consists of a graphite anode placed parallel to the platinum cathode with 5 cm distance. An efficient exfoliation of graphite in presence of H<sub>2</sub>O<sub>2</sub> was observed (Figure 1b). The optimal exfoliation conditions were determined to be 3.0 M NaOH (aq), 130 mM H<sub>2</sub>O<sub>2</sub>, and a working bias voltage of 1 V for 10 min and 3 V for 10 min at room temperature (Table S1, Supplementary Information (SI)). Under these conditions, high-quality anodic few-layer graphene (AFLG) is obtained in 95% yield with 3–6 layers (~1–2 nm thickness platelets). However after centrifugal wash-out of large platelets, almost tri-layer AFLG was obtained with 58% yield. On the other hand, very low quantities of graphene formed in the absence of H<sub>2</sub>O<sub>2</sub> (Table S1, SI). Figure 1c shows a photograph of exfoliated AFLG nanosheets directly in electrolyte solution (I) and dispersed in dimethyl formamide (II) after purification (see experiments section). The purification (wash-out) of such a strong base

species is rather easy to compare with other chemicals like ionic-liquids, organic electrolytes. Stable dispersion of AFLG in dimethyl formamide was found over a period of one month. To study the exfoliation trends at the cathode, the graphite anode was replaced with graphite cathode, but no exfoliation was observed. It reveals anodic exfoliation to be essential in our experiments.

Raman spectroscopy is a fast and non-destructive technique for the structural investigation of carbon nanomaterials, specifically for determining defects and ordered/disordered structures of graphene. The intensity ratio of the D band to the G band ( $I_D/I_G$ ) is generally accepted as representative of the defect/disordered carbon structure<sup>38,39</sup>. The Raman spectrum (excitation with a 633 nm laser) of graphite indicates the presence of the D band (disorder mode) at 1337 cm<sup>-1</sup> and a small D' shoulder band at around 1621 cm<sup>-1</sup>, related to the disorder of edge carbons (Figure 2). The G band (at 1581 cm<sup>-1</sup>) is a doubly degenerate (TO and LO) phonon mode (E2g symmetry) related to ordered in-plane sp<sup>2</sup> carbon atoms. The intense 2D band at 2664 cm<sup>-1</sup> originates from a two-phonon double resonance. The Raman measurements of AFLG show a slight shift of all bands (D band at 1338 cm<sup>-1</sup>, D' shoulder band at 1615 cm<sup>-1</sup>, G band at 1578 cm<sup>-1</sup> and 2D band at 2668 cm<sup>-1</sup>). The measured  $I_D/I_G$  values of graphite and AFLG are 0.54 and 0.67 respectively. Increasing the  $I_D/I_G$  value of AFLG suggests that the oxidation of graphite introduces a few oxygen functional groups during the exfoliation process and thus causes a partial disorder at carbon edges. Insertion of oxygen functional groups into AFLG was further evidenced by X-ray photoelectron spectroscopy (XPS) studies as described in the later stages. Those Raman studies demonstrate our products AFLG are quite similar to those prepared in ionic liquid using 15 V as reported in the literature<sup>14</sup>. High-quality AFLG was produced using our method even at low operational voltage under mild conditions.

Transmission electron microscopy (TEM) images of exfoliated AFLG are shown in Figure 3. A low-magnification TEM image of an AFLG nanosheet on lacy\_carbon is shown in Figure 3a. The selected area image from Figure 3b is shown in Figure 3c, which reveals the defect-free areas of graphene. High-resolution TEM (HR-TEM) analysis of AFLG indicates the presence of large  $\pi$ -network domains. The corresponding hexagonal carbon lattice patterns of the electron diffraction reveal the presence of sp<sup>2</sup>-bonded carbon frameworks with few defects (Figure 3d). A systematic investigation on the statistical distribution of the graphene sheet layers was conducted via careful examination of large number of TEM micrographs obtained from HR-TEM. The data reveals that the as prepared AFLG (before centrifugal wash-out of large platelets) consists of few-layer graphene such as 55% tri-layered graphene sheets, 25% four-layered graphene sheets, 15% five-layered graphene sheets and 5% six-layered graphene sheets (Figures 3e and 3f; Figure S2, SI). After centrifugal wash-out of large platelets, almost tri-layer AFLG is observed. The measured lattice spacing is about 0.35 nm, which is

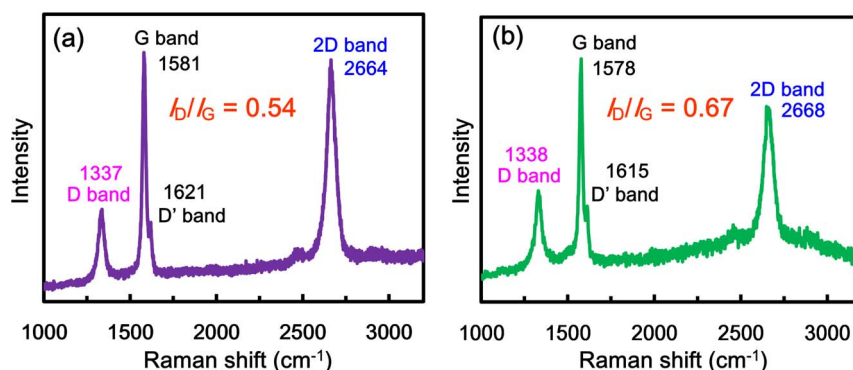


**Figure 2** | Raman spectrum of (a) graphite and (b) exfoliated AFLG, indicating high-quality, few-layer graphene.

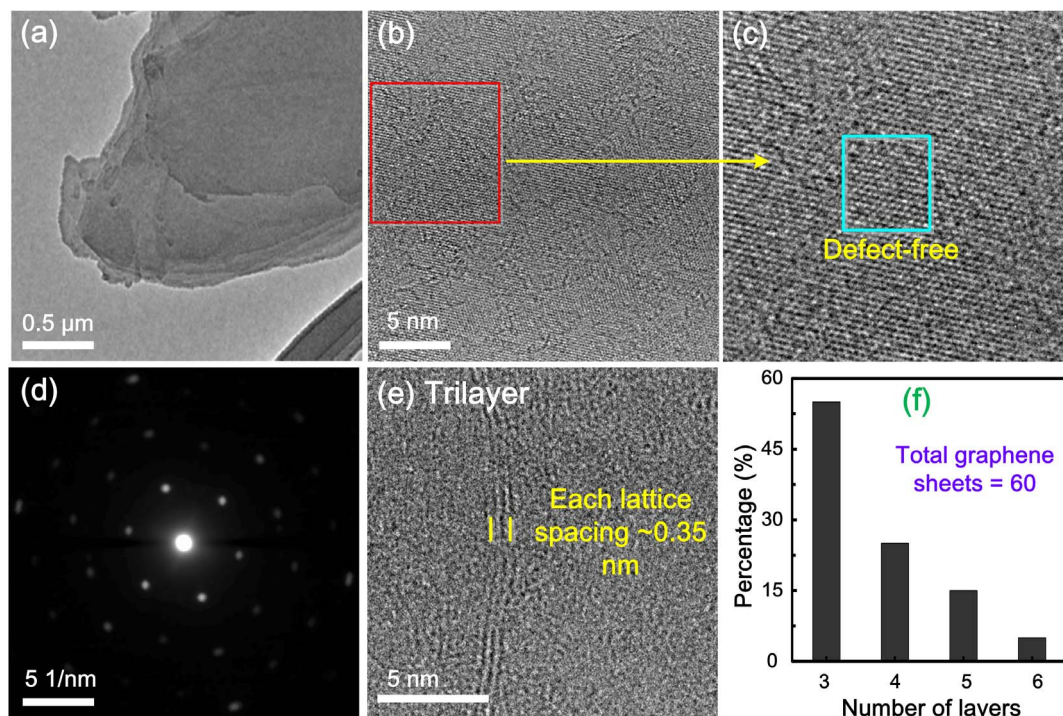


**Figure 3 | TEM characterizations.** (a) low-magnification TEM image of AFLG nanosheet on lacy\_carbon; (b) HR-TEM image of AFLG; (c) selected area image from (b) which contains defect-free areas of graphene; (d) corresponding selected area electron diffraction pattern of carbon lattice; (e) HR-TEM image of tri-layer graphene, (f) distribution of the number of graphene sheet layers before centrifugation.

consistent with that reported in the literature<sup>14</sup> and indicates the insertion of fewer oxygen functional groups during the exfoliation process. The symmetric 2D band ( $2668\text{ cm}^{-1}$ ) of AFLG in the Raman spectrum implies the presence of few-layer graphene<sup>40</sup>. Thus, the atomic structure of  $\pi$ -network domains and the nanoscale morphology of AFLG were analyzed.

The nature of carbon, oxygen bonds, and the level of oxygen introduced into the exfoliated AFLG were analyzed using XPS (Figure 4). The wide-scan XPS spectra of graphite and AFLG confirm the presence of carbon and oxygen (Figure 4a). The carbon to oxygen ratio (C/O) of starting graphite was 98.5:1.5. During the electrochemical exfoliation of AFLG, a low quantity of oxygen functional groups was inserted (C/O = 94.5:5.5). The C1s core levels of graphite and AFLG were analyzed and numerically fitted with Gaussian functions. The C1s spectra of both samples are asymmetric, further indicating that both samples contained oxygen functional groups.

The slightly varied C1s band intensities of graphite (Figure 4b) and AFLG (Figure 4c) indicate that only few oxygen functional groups were inserted during the exfoliation process. The C1s spectra of graphite and AFLG suggest that the bands corresponding to graphitic carbon (C-C) bonds and C-OH bonds of AFLG are almost identical to those of the graphite sample (located at 284.8 eV and 285.9 eV, respectively), which is consistent with values reported in the literature<sup>41–43</sup>. These results suggest the highly graphitic nature of AFLG. Thus, the different structures and composition of graphite and AFLG were confirmed.

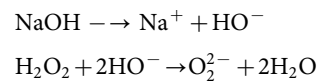
The Fourier transform infrared (FT-IR) spectra (Figure 4d) of graphite and AFLG show peaks at around  $1000\text{ cm}^{-1}$  (C-O stretching),  $1400\text{ cm}^{-1}$  (CO-H bending),  $3342\text{ cm}^{-1}$  (CO-H stretching), and  $1584\text{ cm}^{-1}$  (C=C stretching), corresponding to the hydroxyl functional group<sup>44</sup> and  $\pi$ -network domains respectively. The similar intensities in both the spectra indicate that a very small quantity of the oxygen functional groups was inserted into AFLG during the exfoliation process. The FT-IR results are in good agreement with the XPS results. Additionally, cyclic voltammetry (Figure S3, SI),

thermo gravimetric analysis (Figure S4, SI) studies of AFLG proved that it is essentially graphene, not graphene oxide.

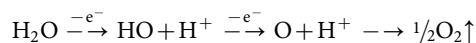
## Discussion

The exfoliation mechanism was examined to understand the role of  $\text{H}_2\text{O}_2$  in the electrochemical exfoliation process. A possible exfoliation mechanism based on the experimental results and published literature<sup>14,30,45</sup> is proposed. A schematic representation of the proposed electrochemical exfoliation mechanism is shown in Figure 5.

- (a) The aqueous solution of NaOH, which contains  $\text{HO}^-$  ions, reacts with  $\text{H}_2\text{O}_2$  to form highly nucleophilic  $\text{O}_2^{2-}$  ions<sup>46,47</sup>.



- (b) Thus,  $\text{O}_2^{2-}$  ions can intercalate into graphite sheets to form graphene layers (AFLG) by exfoliation. Similar intercalation of  $\text{O}_2^{2-}$  ions into graphite has been reported in previous papers<sup>48,49</sup>, where sodium metal in presence of oxygen was used to prepare  $\text{O}_2^{2-}$  ions. Obviously, using sodium metal is dangerous.
- (c) Electrochemical potentials (electric field force) assist the exfoliation, which is supported by the literature<sup>15</sup>. The potential also helps anodic reactions. Thus, the properties of exfoliated graphene can be controlled by changing the potential<sup>50</sup>.
- (d) Additionally, hydroxyl (OH) and oxygen (O) radicals may be generated from the anodic oxidation<sup>14</sup> of water.



- (e) Radicals are powerful, highly reactive, and non-selective chemical oxidants<sup>51</sup>. Thus, the oxidation of graphite edge planes by radicals opens up the edge sheets, facilitating the intercalation

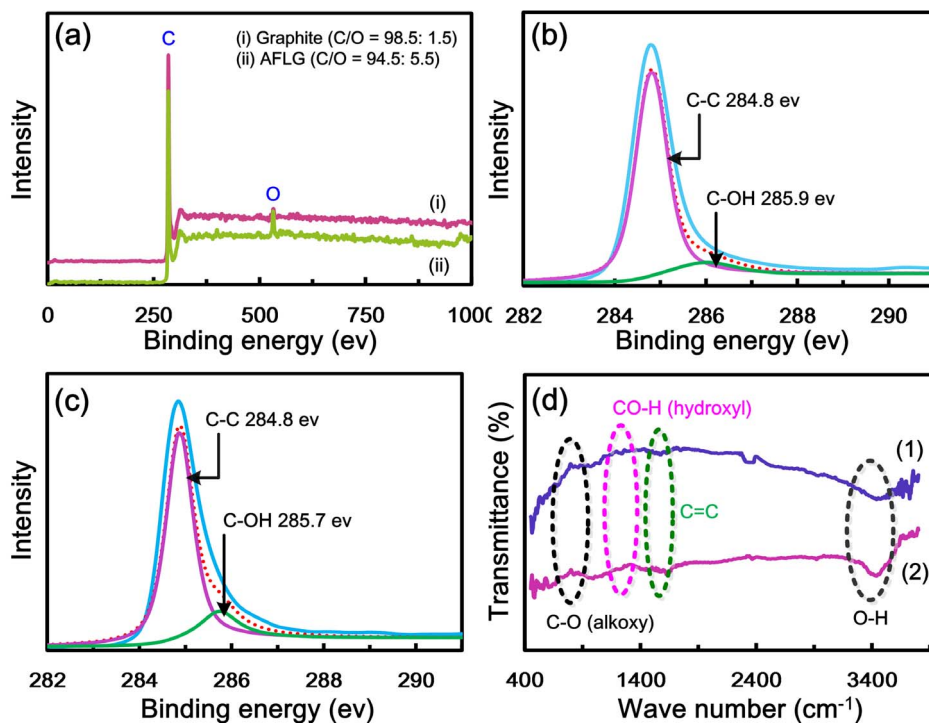


**Figure 4** | XPS characterizations. (a) wide-scan XPS spectra of (i) graphite and (ii) AFLG. C1s XPS spectra of (b) graphite and (c) exfoliated AFLG, (d) FT-IR spectra of (1) graphite and (2) AFLG.

of  $\text{HO}^-$  and  $\text{O}_2^{2-}$  ions, and subsequently promotes depolarization and the subsequent, expansion of the graphite anode<sup>52,53</sup>.

In the absence of  $\text{H}_2\text{O}_2$ , the low-nucleophilicity  $\text{HO}^-$  ions do not effectively intercalate and/or have poor interactions with graphite domains even under harsh conditions (5 V, 25 min). The resulting weak expansion of graphite sheets gives poor yields. In the presence of  $\text{H}_2\text{O}_2$ , even under mild reaction conditions (1 V for 10 min, then 3 V for 10 min), an efficient exfoliation of graphite was observed. Thus,  $\text{H}_2\text{O}_2$  plays a crucial role in the electrochemical exfoliation of graphite. It is believed that the proposed mechanism is useful for controlling/manipulating the properties of exfoliated graphene. A systematic analysis and comparison study proves that the proposed method is superior over reported methods (see Table S2, S3, SI for more discussion).

In conclusion, the proposed method has a significant number of advantages over reported methods for the synthesis of AFLG, including (a) simple reaction set up, (b) ambient reaction conditions, (c) easy operational procedure, (d) an efficient (effective exfoliation and inhibition of graphene sheets restacking), facile (low operating voltage 1 V for 10 min, then 3 V for 10 min), and fast (20 min) approach, (e) low concentration/cheap reagents (and thus low cost) of reagents, (f) single-step, environmentally-friendly and mild (relatively mild reagents), soft processing approach, (g) NaOH-induced

reduction of preformed oxygen functional groups, and (h) stable dispersions of high-quality few-layer graphene nanosheets, (i) possible to use cheaper graphite sources such as graphite powders and graphite flakes. A reasonable exfoliation mechanism for the synthesis of AFLG that considers the crucial role of hydrogen peroxide was proposed. The present method is an excellent choice for graphene material synthesis. Moreover it will provide fabrication of graphene ink with an additional easy purification step. They are significant advantageous for future applications.

## Methods

**Experiments.** All other chemicals were purchased from Sigma-Aldrich and used directly without further purification. High purity graphite rods (99.9995%, 6.15 mm diameter, 152 mm length) were purchased from the Alfa Aesar. All solvents used in this study were HPLC grade. Aqueous solutions were purified with Milli-Q water (>18.2 M $\Omega$ ) from a Roda purification system (Te Chen Co. Ltd). In the electrochemical experiments, graphite rod was inserted as anode into the electrolytic solution, placed parallel to the Pt sheet as counter-electrode with 5 cm separation. A regulated DC power supply potentiostat system (TES-6200, USA) was used to maintain different static potentials (1.0–10 V) between two electrodes. All experiments were performed at ambient reaction conditions. In our experiments, different quantities of NaOH was dissolved in water (75 ml), then added different quantity of  $\text{H}_2\text{O}_2$  (Table S1). After appropriate time, corrosion of the graphite anode and subsequent dispersion of black precipitate in electrolyte solution was gradually observed. The precipitate was collected from the electrochemical cell. To prepare AFLG sheet suspension, the exfoliated graphene sheets were collected by using

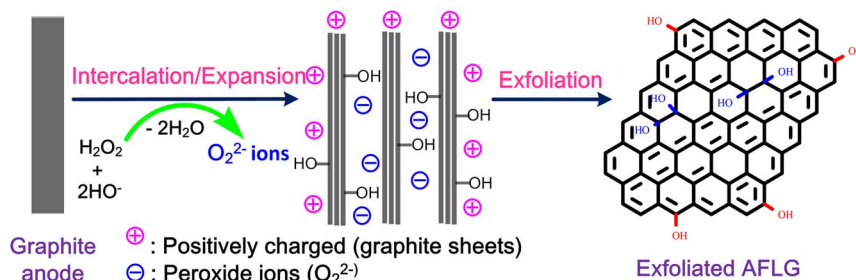


**Figure 5** | Schematics of proposed exfoliation mechanism.



100 nm porous filters, washed with excess of DI water, diluted HCl, DI water, then with ethanol by vacuum filtration and dried in oven for 2 h at 60°C under vacuum. The dry sheets were dispersed into dimethyl formamide by gentle water-bath sonication over 10 min. The resulted supernatant suspension was used for further characterizations.

**Characterizations.** The nanostructure and surface morphology of exfoliated AFLG was investigated by HR-TEM (JEOL, JSM 2100F) at an acceleration voltage of 200 kV. The XPS measurements of graphite, AFLG, were conducted (PHI Quantera SXM ULVAC Inc., Kanagawa, Japan) to analyze the binding energies of carbon, oxygen. The Raman spectra were recorded by a confocal micro-Raman spectrometer (Renishaw inVia) with an argon ion laser at an excitation wavelength of 633 nm and 8 mW/cm<sup>2</sup> laser power. The Si peak at 520 cm<sup>-1</sup> was used as reference for wavenumber calibration. FT-IR spectroscopy with a range of 400 to 4000 cm<sup>-1</sup> was carried on a VERTEX 70 Fourier transforms infrared spectrometer (Bruker, Germany) using KBr disc method. The cyclic voltammetry experiments were conducted using an Eco Chemie Autolab potentiostat/galvanostat. Thermo gravimetric analysis (Perkin-Elmer TGA 7) experiments were conducted from ambient temperature to 500°C with a heating rate 10°C/min under nitrogen atmosphere. The samples for TEM analysis was prepared by drop-casting on lacy carbon-coated Cu grid and dried at 60°C for 30 min. Raman spectroscopy and XPS analysis samples were prepared by deposition of re-dispersed sample onto a glass substrate. The XPS analysis was conducted using pre-sputtered samples.

- Park, S. & Ruoff, R. S. Chemical methods for the production of graphenes. *Nat. Nanotechnol.* **4**, 217–224 (2009).
- Zhu, C.-H., Lu, Y., Peng, J., Chen, J. & Yu, S.-H. Photothermally sensitive poly(*N*-isopropylacrylamide)/graphene oxide nanocomposite hydrogels as remote light-controlled liquid microvalves. *Adv. Funct. Mater.* **22**, 4017–4022 (2012).
- Novoselov, K. S. *et al.* A roadmap for graphene. *Nature* **490**, 192–200 (2012).
- Bonaccorso, F. *et al.* Production and processing of graphene and 2 d crystals. *Mater. Today* **15**, 564–589 (2012).
- Ruoff, R. S. Personal perspectives on graphene: New graphene-related materials on the horizon. *MRS Bulletin* **37**, 1314–1318 (2012).
- Hawaladar, R. *et al.* Large-area high-throughput synthesis of monolayer graphene sheet by hot filament thermal chemical vapor deposition. *Sci. Rep.* **2**, 682–690 (2012).
- Yoon, J.-C., Lee, J.-S., Kim, S.-I., Kim, K.-H. & Jang, J.-H. Three-dimensional graphene nano-networks with high quality and mass production capability via precursor-assisted chemical vapor deposition. *Sci. Rep.* **3**, 1788–1795 (2013).
- Hasan, T. *et al.* Solution-phase exfoliation of graphite for ultrafast photonics. *Phys. Status Solidi B* **247**, 2953–2957 (2010).
- Chabot, V., Kim, B., Sloper, B., Tzoganakis, C. & Yu, A. High yield production and purification of few layer graphene by gum arabic assisted physical sonication. *Sci. Rep.* **3**, 1378–1384 (2013).
- Hu, H., Zhao, Z., Wan, W., Gogotsi, Y. & Qiu, J. Ultralight and highly compressible graphene aerogels. *Adv. Mater.* **25**, 2219–2223 (2013).
- Hu, H., Zhao, Z., Zhou, Q., Gogotsi, Y. & Qiu, J. The role of microwave absorption on formation of graphene from graphite oxide. *Carbon* **50**, 3267–3273 (2012).
- Marago, O. M. *et al.* Brownian motion of graphene. *ACS Nano* **4**, 7515–7523 (2010).
- Wang, X. *et al.* Solution-processable graphene nanomeshes with controlled pore structures. *Sci. Rep.* **3**, 1996–2000 (2013).
- Lu, J. *et al.* One-pot synthesis of fluorescent carbon nanoribbons, nanoparticles, and graphene by the exfoliation of graphite in ionic liquids. *ACS Nano* **3**, 2367–2375 (2009).
- Mao, M. *et al.* Simultaneous electrochemical synthesis of few-layer graphene flakes on both electrodes in protic ionic liquids. *Chem. Commun.* **49**, 5301–5303 (2013).
- Liu, N. *et al.* One-step ionic-liquid-assisted electrochemical synthesis of ionic-liquid-functionalized graphene sheets directly from graphite. *Adv. Funct. Mater.* **18**, 1518–1525 (2008).
- Su, C.-Y. *et al.* High-quality thin graphene films from fast electrochemical exfoliation. *ACS Nano* **5**, 2332–2339 (2011).
- Xia, Z. Y. *et al.* The exfoliation of graphene in liquids by electrochemical, chemical, and sonication-assisted techniques: A nanoscale study. *Adv. Funct. Mater.* **23**, 4684–4693 (2013).
- Morales, G. M. *et al.* High-quality few layer graphene produced by electrochemical intercalation and microwave-assisted expansion of graphite. *Carbon* **49**, 2809–2816 (2011).
- Liu, J. *et al.* Improved synthesis of graphene flakes from the multiple electrochemical exfoliation of graphite rod. *Nano Energy* **2**, 377–386 (2013).
- Huang, H. *et al.* Highly efficient electrolytic exfoliation of graphite into graphene sheets based on Li ions intercalation-expansion-microexplosion mechanism. *J. Mater. Chem.* **22**, 10452–10456 (2012).
- Wang, J., Manga, K. K., Bao, Q. & Loh, K. P. High-yield synthesis of few-layer graphene flakes through electrochemical expansion of graphite in propylene carbonate electrolyte. *J. Am. Chem. Soc.* **133**, 8888–8891 (2011).
- Zhong, Y. L. & Swager, T. M. Enhanced electrochemical expansion of graphite for *in situ* electrochemical functionalization. *J. Am. Chem. Soc.* **134**, 17896–17899 (2012).
- Alanyalioglu, M., Segura, J. J., Oró-Solé, J. & Casañ-Pastor, N. The synthesis of graphene sheets with controlled thickness and order using surfactant-assisted electrochemical processes. *Carbon* **50**, 142–152 (2012).
- Zhou, M. *et al.* Few-layer graphene obtained by electrochemical exfoliation of graphite cathode. *Chem. Phys. Lett.* **572**, 61–65 (2013).
- Lu, W. *et al.* High-yield, large-scale production of few-layer graphene flakes within seconds: Using chlorosulfonic acid and H<sub>2</sub>O<sub>2</sub> as exfoliating agents. *J. Mater. Chem.* **22**, 8775–8777 (2012).
- Vona, M. L. D. *et al.* A simple new route to covalent organic/inorganic hybrid proton exchange polymeric membranes. *Chem. Mater.* **18**, 69–75 (2006).
- Behabtu, N. *et al.* Spontaneous high-concentration dispersions and liquid crystals of graphene. *Nat. Nanotechnol.* **5**, 406–411 (2010).
- Chen, X. *et al.* Structure study of cellulose fibers wet-spun from environmentally friendly NaOH/urea aqueous solutions. *Biomacromolecules* **8**, 1918–1926 (2007).
- Kuila, T., Khanra, P., Kim, N. H., Lim, J. K. & Lee, J. H. Effects of sodium hydroxide on the yield and electrochemical performance of sulfonated poly(ether-ether-ketone) functionalized graphene. *J. Mater. Chem. A* **1**, 9294–9302 (2013).
- Boronat, M., Corma, A., Renz, M., Sastre, G. & Viruela, P. M. A multisite molecular mechanism for Baeyer-Villiger oxidations on solid catalysts using environmental-friendly H<sub>2</sub>O<sub>2</sub> as oxidant. *Chem. Eur. J.* **11**, 6905–6915 (2005).
- Yoshimura, M. & Livage, J. Soft processing for advanced inorganic materials. *MRS Bulletin Special Issue* **25**, 12–13 (2000).
- Yoshimura, M. Importance of soft solution processing for advanced inorganic materials. *J. Mater. Res.* **13**, 796–802 (1998).
- Yoshimura, M. Soft solution processing: Concept and realization of direct fabrication of shaped ceramics (nano-crystals, whiskers, films, and/or patterns) in solutions without post-firing. *J. Mater. Sci.* **41**, 1299–1306 (2006).
- Krtlić, P., Fattakhova, D. & Yoshimura, M. Mechanism of soft solution processing formation of alkaline earth metal tungstates: An electrochemical and *in situ* AFM study. *J. Solid State Electrochem.* **6**, 367–373 (2002).
- Lemmer, K., Mielke, M., Pauli, G. & Beekes, M. Decontamination of surgical instruments from prion proteins: *In vitro* studies on the detachment, destabilization and degradation of PrPSc bound to steel surfaces. *J. Gen. Virol.* **85**, 3805–3816 (2004).
- Ding, Y., Zhao, W., Song, W., Zhang, Z. & Ma, B. Mild and recyclable catalytic oxidation of pyridines to N-oxides with H<sub>2</sub>O<sub>2</sub> in water mediated by a vanadium-substituted polyoxometalate. *Green Chem.* **13**, 1486–1489 (2011).
- Ferrari, C. & Robertson, J. Interpretation of Raman spectra of disordered and amorphous carbon. *Phys. Rev. B* **61**, 14095–14107 (2000).
- Cancado, L. G. *et al.* Quantifying defects in graphene via Raman spectroscopy at different excitation energies. *Nano Lett.* **11**, 3190–3196 (2011).
- Ferrari, A. C. *et al.* Raman spectrum of graphene and graphene layers. *Phys. Rev. Lett.* **97**, 187401–187404 (2006).
- Li, Y., Zijl, M. V., Chiang, S. & Pan, N. KOH modified graphene nanosheets for supercapacitor electrodes. *J. Power Sources* **196**, 6003–6006 (2011).
- Park, S. *et al.* Aqueous suspension and characterization of chemically modified graphene sheets. *Chem. Mater.* **20**, 6592–6594 (2008).
- Yumitori, S. Correlation of C1s chemical state intensities with the O1s intensity in the XPS analysis of anodically oxidized glass-like carbon samples. *J. Mater. Sci.* **35**, 139–146 (2000).
- Zhu, G.-X., Wei, X.-W. & Jiang, S. A facile route to carbon-coated nickel-based metal nanoparticles. *J. Mater. Chem.* **17**, 2301–2306 (2007).
- Lee, J. H. *et al.* One-step exfoliation synthesis of easily soluble graphite and transparent conducting graphene sheets. *Adv. Mater.* **21**, 4383–4387 (2009).
- Campos-Martin, J. M., Blanco-Brieva, G. & Fierro, J. L. G. Hydrogen peroxide synthesis: An outlook beyond the anthraquinone process. *Angew. Chem. Int. Ed.* **45**, 6962–6984 (2006).
- Mei, J., Carsch, K. M., Freitag, C. R., Gunnoe, T. B. & Cundari, T. R. Variable pathways for oxygen atom insertion into metal-carbon bonds: The case of Cp\*W(O)<sub>2</sub>(CH<sub>2</sub>SiMe<sub>3</sub>). *J. Am. Chem. Soc.* **135**, 424–435 (2013).
- Spyrou, K. *et al.* A novel route towards high quality fullerene-pillared graphene. *Carbon* **61**, 313–320 (2013).
- Pruvost, S., Herold, C., Herold, A. & Lagrange, P. Co-intercalation into graphite of lithium and sodium with an alkaline earth metal. *Carbon* **42**, 1825–1831 (2004).
- Novoselov, K. S. *et al.* Electric field effect in atomically thin carbon films. *Science* **306**, 666–669 (2004).
- Buxton, G. V., Greenstock, C. L., Helman, W. P. & Ross, A. B. Critical review of rate constants for reactions of hydrated electrons, hydrogen atoms and hydroxyl radicals (·OH/·O<sup>-</sup> in aqueous solution). *J. Phys. Chem. Ref. Data* **17**, 513–886 (1988).
- Seel, J. A. & Dahn, J. R. Electrochemical intercalation of PF<sub>6</sub> into graphite. *J. Electrochem. Soc.* **147**, 892–898 (2000).
- Katinaonkul, W. & Lerner, M. M. Graphite intercalation compounds with large fluoroanions. *J. Fluorine Chem.* **128**, 332–335 (2007).

## Acknowledgments

The authors would like to thank professors Jiunn-Der Liao, Jyh-Ming Ting, Jih-Jen Wu, Yuh-Lang Lee and Mario Hofmann and Dr. Venkatesh Shanmugam, Dr. Wan-Hsien Lin and Ms Pei-Ru So and Hsun-Wei Cho for their support in this research. This work was supported by National Cheng Kung University, Taiwan.



### Author contributions

M.Y. and K.S.R. performed the experimental research, data analysis, and manuscript preparation. J.S. and Y.-F.L. also contributed to the experimental researches, data interpretation and discussion.

### Additional information

Supplementary information accompanies this paper at <http://www.nature.com/scientificreports>

**Competing financial interests:** The authors declare no competing financial interests.

**How to cite this article:** Sanjeeva Rao, K., Senthilnathan, J., Liu, Y.-F. & Yoshimura, M. Role of Peroxide Ions in Formation of Graphene Nanosheets by Electrochemical Exfoliation of Graphite. *Sci. Rep.* 4, 4237; DOI:10.1038/srep04237 (2014).



This work is licensed under a Creative Commons Attribution-NonCommercial-NoDerivs 3.0 Unported license. To view a copy of this license, visit <http://creativecommons.org/licenses/by-nc-nd/3.0>